INTERNAL FRICTION IN ALPHA BRASS

by

James E. Steedly, Jr.

A Thesis Submitted to the Faculty of the

DEPARTMENT OF METALLURGICAL ENGINEERING

In Partial Fulfillment of the Requirements
For the Degree of

MASTER OF SCIENCE

In the Graduate College

THE UNIVERSITY OF ARIZONA

1965

STATEMENT BY AUTHOR

This thesis has been submitted in partial fulfillment of the requirements for an advanced degree at The University of Arizona and is deposited in the University Library to be made available to borrowers under rules of the Library.

Brief quotations from this thesis are allowable without special permission, provided that accurate acknowledgment of source is made. Requests for permission for extended quotation from or reproduction of this manuscript in whole or in part may be granted by the head of the major department or the Dean of the Graduate College when in his judgment, the proposed use of the material is in the interests of scholarship. In all other instances, however, permission must be obtained from the author.

SIGNED: James E. Steedly

APPROVAL BY THESIS DIRECTOR

This thesis has been approved on the date shown below:

C. T. Tomizuka

C. T. TOMIZUKA
Professor of Physics

May 10, 1965
Date

ACKNOWLEDGEMENTS

The author expresses his appreciation to the staffs of the Department of Physics and the Department of Metallurgical Engineering for their help on this thesis. He is expecially indebted to his Co-director of thesis, Dr. Carl T. Tomizuka, for his guidance and assistance and to his Director of thesis, Dr. Louis J. Demer, for his support. In addition, the author wishes to acknowledge the contribution of Mr. George Rosevere for making chemical analyses and the assistance of Mr. Rick Roberts for helping make internal friction measurements. Lastly, he thanks Capt. Roger J. Austin for his helpful comments and suggestions on this thesis.

TABLE OF CONTENTS

LIST OF ILLUSTRATIONS

LIST OF TABLES

ABSTRACT

An anelastic study of the stress-induced ordering phenomenon in metallic substitutional solid solutions, known as the "Zener relaxation effect," was made on an alpha brass alloy. Relaxation times for the Zener peak were obtained on a 13 atomic percent Zn-87 atomic percent Cu alloy, using low frequency internal friction and elastic after-effect measurements. The relaxation time is expressed by the Arrhenius equation

$$\tau = 4.0 \times 10^{-15} e^{40,900/RT}$$

An activation energy of 40.9 kcal/mole was obtained for the stress-induced ordering process. Results for this study were compared with other internal friction investigations and diffusion data on the alpha brass system. The results are discussed in connection with present theories of stress-induced ordering of substutional solid solutions.

INTRODUCTION

Anelastic studies have become very important in recent years for studying the behavior of materials, especially metal alloy systems. Anelastic measurements have added a new dimension to the experimental techniques for examining metals (1). The method has been very useful in studying the properties of metals and in solving many problems in physical metallurgy which previously could not be resolved. However, the technique does have certain limitations which must be recognized before an attempt is made to apply it to the solution of a particular problem. It is necessary to have a clear understanding of anelasticity and the sources which give rise to anelastic behavior in a material.

All metals behave nonelastically in the sense that stress and strain are not single valued functions of one another even at low stress levels. This deviation from perfect elasticity of metals at low stress levels (below the plastic region of deformation where no permanent set occurs) is called anelasticity. When a constant stress is applied to a metal, it is followed by one or more types of relaxation, resulting in gradual creep of the metal which is usually recoverable.

Two types of anelastic measurements, internal friction and the elastic after-effect, were used in this investigation to study atomic mobility in an alpha brass alloy. When a metal specimen is caused to oscillate, it will lose its vibrational energy even though it is completely isolated from its surroundings. This energy loss is due to what is commonly called internal friction, one of the most often-measured anelastic effects. An inverted torsional pendulum apparatus was employed in this study to make internal friction measurements at relaxation times of the order of one second. The elastic after-effect was used to measure relaxation times greater than a few seconds.

The anelastic relaxation process investigated in this study was the stress-induced ordering phenomenon in metallic substitutional solid solutions. This is commonly called the "Zener relaxation effect." Since the relaxation process involves the movement of substitutional atoms within the lattice, it is similar to the diffusion process. There are several advantages of using anelastic measurements to study atomic mobility in alloys. Diffusion experiments are limited to high temperatures and long times, while anelastic measurements can be made in a short time and at much lower temperatures. By using the data of both methods, one may obtain activation energies and diffusion coefficients over a much wider temperature range.

The alpha brass system was chosen for this investigation because there have been some discrepancies (2) between the activation energies determined from diffusion experiments and those determined from anelastic experiments. The purpose of this study was to compare the results of internal friction and elastic after-effect measurements for an alpha brass alloy with available diffusion data. The experimental results are discussed in light of existing theories of stress-induced ordering with various conclusions drawn and recommendations made from the work.

THEORY OF ANELASTICITY

The classical theory of elasticity is based on Hooke's law, which applies to perfectly elastic materials. The behavior of stress and strain for perfectly elastic materials is independent of time and is given by the following equation

$$\sigma = M\varepsilon \qquad [1]$$

where σ is the stress, ε is the strain, and M is the modulus of elasticity. Since real materials are not perfectly elastic and exhibit elastic after-effects, Eqn. [1] does not adequately describe the behavior of real materials. When a force is applied to a real solid, an elastic displacement occurs which is followed by various types of relaxations resulting in gradual creep of the material with time. Numerous attempts have been made to construct a model for representing the mechanical characteristics of real materials.

Standard Linear Solid*

The "standard linear solid" was proposed by Zener (3, 4) to represent the mechanical behavior of real solids. The equation relating stress and strain for the "standard linear solid" is given by

$$\sigma + \tau_\varepsilon \frac{d\sigma}{dt} = M_R\left(\varepsilon + \tau_\sigma \frac{d\varepsilon}{dt}\right) \qquad [2]$$

where t is the time, τ_ε is the time of relaxation of stress under constant strain, τ_σ is the time of relaxation of strain under constant stress, and M_R is the relaxed elastic modulus (ratio of stress to strain after all relaxation has occurred).

---

* See APPENDIX A for details of equations in this section.

When a constant stress σ_o is suddenly applied to a standard linear solid, the solution to Eqn. [2] becomes

$$\varepsilon = \frac{\sigma_o}{M_R} + \left(\varepsilon_o - \frac{\sigma_o}{M_R}\right) e^{-t/\tau_\sigma} \qquad [3]$$

The strain immediately rises to a value ε_o and then increases gradually with the time of relaxation τ_σ to its equilibrium value, $\varepsilon_\infty = \sigma_o/M_R$, at infinite time as shown in Fig. 1a. After the applied stress is removed, the strain suddenly decreases by an amount ε_o and gradually continues to decrease to zero.

When a constant strain is suddenly applied to a standard linear solid, the solution to Eqn. [2] becomes

$$\sigma = M_R\varepsilon_o + (\sigma_o - M_R\varepsilon_o)\, e^{-t/\tau_\varepsilon} \qquad [4]$$

The stress decays from an initial value of σ_o, with the time of relaxation τ_ε, to its final value, $\sigma_\infty = M_R\varepsilon_o$, at infinite time as shown in Fig. 1b. When the strain is annulled, the stress instantaneously drops by an amount σ_o and then gradually approaches zero.

The relaxed modulus is the ratio of stress to strain after complete relaxation has occurred. If Eqn. [2] is integrated with respect to time over a very short time interval δt during which the stress changes by a finite increment $\Delta\sigma$, then the following relation is obtained between the increments of stress, $\Delta\sigma$, and strain, $\Delta\varepsilon$, as δt approaches zero

$$\tau_\varepsilon \Delta\sigma = M_R \tau_\sigma \Delta\varepsilon \qquad [5]$$

The ratio is $\Delta\sigma/\Delta\varepsilon$, which is denoted by M_u, is called the unrelaxed elastic modulus, since it gives the relation between changes in stress and strain which occur so rapidly that no relaxation has time to take effect. Therefore, Eqn. [5] becomes

$$\frac{M_u}{M_R} = \frac{\tau_\sigma}{\tau_\varepsilon} \qquad [6]$$

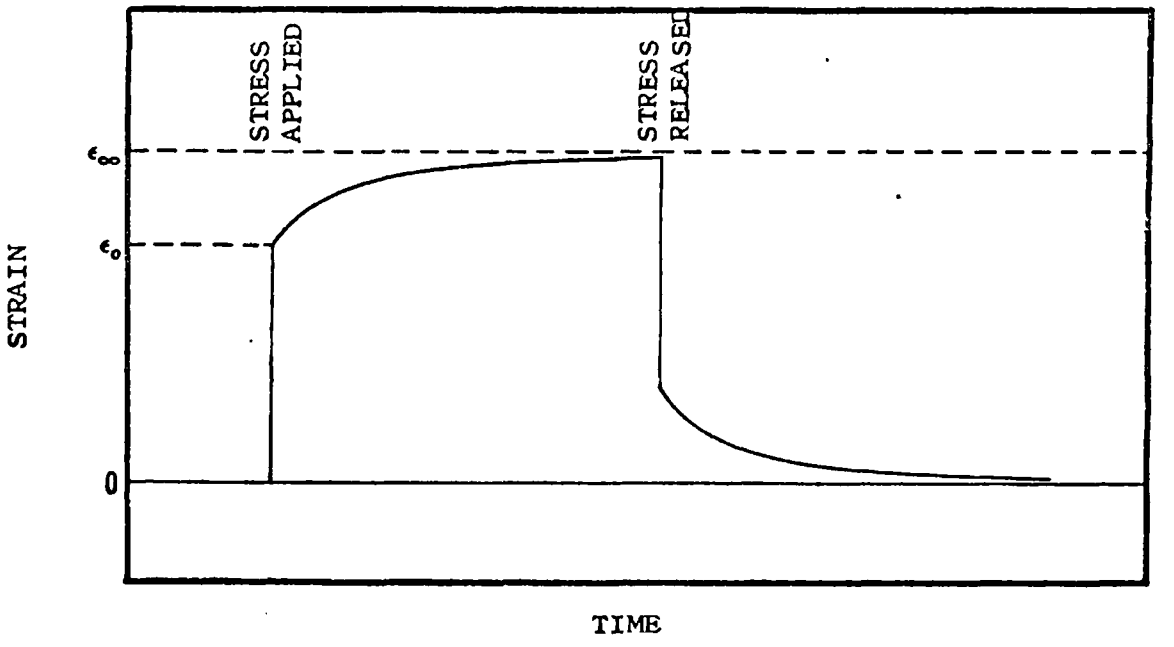

Fig. 1a.--Relaxation of strain under a constant stress (4).

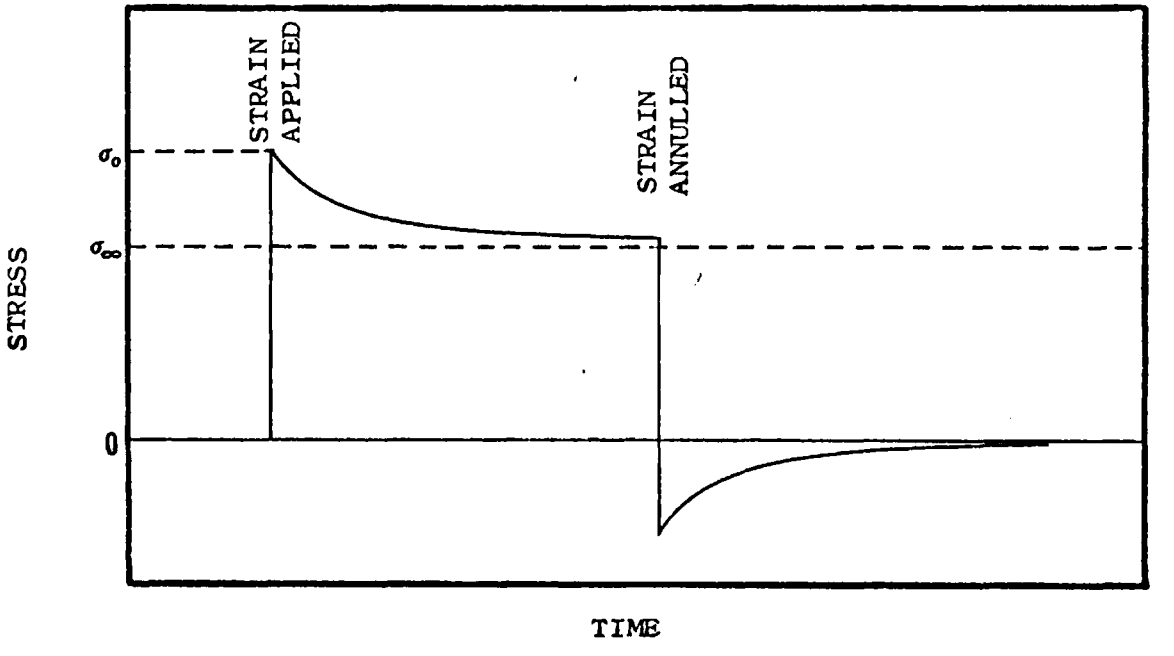

Fig. 1b.--Relaxation of stress under a constant strain (4).

The deviation of the ratio M_R/M_u from unity is a measure of the relative change in stress or in strain which may occur through relaxation.

Internal Friction

It is often experimentally fruitful to investigate anelastic behavior under the conditions of periodic stress and strain (1, 3, 4, 5, 6). The relaxation phenomenon then manifests itself in a phase lag of stress. The tangent of the angle by which strain lags behind stress, a measure of internal friction, is given by

$$\tan \delta = \Delta E \frac{\omega\tau}{1 + (\omega\tau)^2} \qquad [7]^*$$

where ΔE is the relaxation strength, ω is the angular frequency of oscillation, and τ is the mean relaxation time. Eqn. [7] is valid only when $\Delta E << 1$ and gives rise to an internal friction peak with a maximum value of

$$\tan \delta = \frac{\Delta E}{2} \qquad [8]$$

at

$$\omega\tau = 1 \qquad [9]$$

when the phase lag is maximum. The variation of tan δ (internal friction) with frequency is shown in Fig. 2.

The elastic modulus also changes with frequency as shown in Fig. 2. At very low frequencies where $\omega\tau << 1$, there is no phase lag between stress and strain since there is sufficient time during each periodic cycle for complete relaxation to take place. Thus, the elastic modulus becomes the relaxed modulus, M_R, as shown in Fig. 2. At very high frequency where $\omega\tau >> 1$, there is no phase lag because one oscillation is too fast for relaxation to occur. In this case, the elastic modulus approaches the unrelaxed modulus, M_u. The rate of change of

*See APPENDIX B for derivation of Eqn. [7].

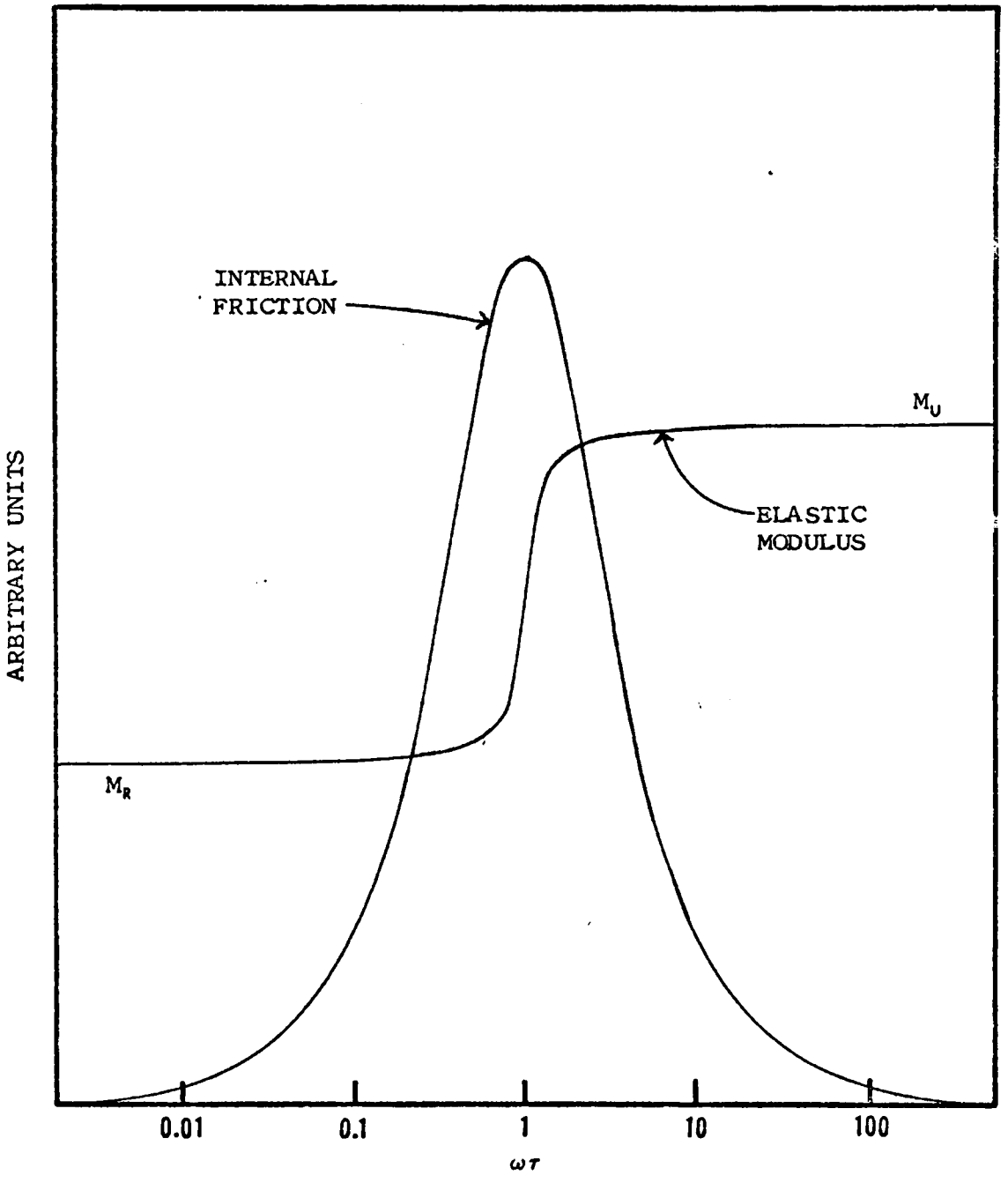

Fig. 2.--Variation of internal friction and elastic modulus with frequency and relaxation time (3,4).

the elastic modulus is a maximum at $\omega = 1$ (inflection point for elastic modulus curve in Fig. 2) where the internal friction is also a maximum. The elastic modulus is proportional to the square of the frequency of specimen vibration. The inflection point for the change in the elastic modulus can be determined experimentally from a plot of temperature versus the frequency squared.

The tangent of the phase lag angle, δ, is usually small and is often represented by the symbol Q^{-1}, by analogy to damping in electrical circuits (1). The internal friction can be determined directly by measuring the phase lag angle, δ, but may be measured indirectly in most experiments, since the internal friction is small compared to unity. One experimental method is to observe the free decay in amplitude of vibration of a system set into oscillation. Energy is dissipated in a freely vibrating sample which results in a gradual decrease of the amplitude of vibration. The internal friction may then be expressed in terms of the logarithmic decrement (1, 3) by the following equation

$$Q^{-1} = \tan \delta = \frac{\text{logarithmic decrement}}{\pi} \qquad [10]$$

where the logarithmic decrement is defined as the natural logarithm of the ratio of successive amplitudes of oscillation. Eqn. [10] holds true only for small values of internal friction. In actual experiment, it is common to observe the time, t, required for the amplitude of vibration to decay to 1/N of its original value (used in this study). Therefore, Eqn. [10] becomes

$$\tan \delta = \frac{\ell n \ N}{\pi \omega t} \qquad [11]^*$$

where ω is the frequency of vibration.

Regions of high internal friction or relaxation peaks which are characterized by a single relaxation time, τ, at a given temperature may be obtained by varying the frequency with a constant τ. Each

*See APPENDIX C for derivation of Eqn. [11].

relaxation peak obtained is caused by the effect of a physical mechanism operating within the metal. Usually it is easier experimentally to hold the frequency constant and vary the relaxation time. This is easily done when the relaxation time obeys the Arrhenius equation.

$$\tau = \tau_o e^{\Delta H/RT} \qquad [12]$$

where τ_o is a constant, ΔH is the heat of activation energy for the relaxation process, R is the gas constant, and T is the absolute temperature. In this case, the relaxation peak may be obtained by measuring the intermal friction as a function of temperature. The relaxation time at various temperatures may be obtained by measuring the internal friction as a function of temperature at different frequencies, provided that the order of magnitude of the relaxation time is less than one second.

Elastic After-Effect

The elastic after-effect is used to measure relaxation times greater than a few seconds (7). The specimen is subjected to a stress for sufficient time to establish equilibrium. When the stress is released, the anelastic strain decays exponentially to zero as shown in Fig. 1a. The strain is expressed as a function of time by the following equation

$$\xi = \xi_o e^{-t/\tau} \qquad [13]$$

where ξ is the anelastic strain at time t, τ is the relaxation time, and ξ_o is the total anelastic strain recoverable.

The relaxation time for the elastic after-effect can be determined by several methods. The relaxation time can be taken as the time to reach the inflection point in a plot of log time versus linear strain (used in this study). It can also be found from the slope of a plot for linear time versus log strain. Still another way is to measure the time needed for the anelastic strain to decrease to 1/eth of its initial value. The first method is the easiest for determining the relaxation time, since

it is not necessary to know either the initial deflection of the specimen or the final position after complete relaxation has occurred.

THEORY OF SUBSTITUTIONAL STRESS-INDUCED ORDERING

Anelastic methods have been successfully used in studying the stress-induced ordering phenomenon in substitutional alloys. The stress-induced ordering mechanism was first observed in alpha brass by Zener (8), and subsequently became known as the "Zener relaxation effect." Several theories have been proposed to explain the stress-induced ordering phenomenon in substitutional solid solutions.

Zener's Theory

Zener interpreted the relaxation phenomenon as a reorientation of pairs of adjacent solute atoms in preferential lattice sites (9,10). The solute and solvent atoms of the alloy are assumed to differ in size. If the atoms are arranged at random in a face-centered cubic lattice, the solute atoms will produce an elastic distortion in the lattice which will have cubic symmetry. But, a pair of adjacent solute atoms will no longer have cubic symmetry and cause an elastic distortion along the axis of the pair. The pair axes will be distributed at random over all the permissible crystallographic directions in the absence of an external stress. When a stress is applied to the crystal, the pair axes will rotate to crystallographic directions most closely aligned with the stress direction. A certain time will be required for the reorientation of the pair axes, so that the strain will lag behind the stress. In Zener's theory, the reorientation time of the solute pair is the relaxation time, τ. The temperature variation of the internal friction is explained as follows. At low temperatures (below the internal friction peak) the time of relaxation for the stress induced ordering to establish equilibrium is very long compared with the vibrational period of the applied stress. Therefore, during specimen vibration, the distribution of the atoms remains essentially unaltered and strain is nearly in phase with

stress. Thus, the internal friction is very small. At high temperatures (above the internal friction peak) the time of relaxation for the ordering to reach equilibrium is very short compared with the period of specimen vibration. Since equilibrium is reached almost instantaneously, strain is nearly in phase with stress and the internal friction is very small. Only in some intermediate temperature range where the period of vibration is approximately equal to the period of relaxation does the internal friction become relatively large. In this range the solute atoms tend to order under the applied stress. The strain exhibits maximum lag behind stress, giving rise to an internal friction peak.

Zener's theory explains several important features of the relaxation process. The activation energy for the relaxation process is nearly the same as that for volume self-diffusion in numerous metallic systems. This result is expected since both processes involve atomic migration. Secondly, the relaxation strength varies as the square of the concentration for low solute concentration, indicating that the process involves a pair of solute atoms. This also explains why solute concentrations of 10 per cent or more are needed to get an observable Zener relaxation. However, Zener's theory has several weaknesses. The theory does not account for the effect of next-nearest neighbors which may contribute to the relaxation process, tendancies toward short-range ordering, and segregation in the solid solution. It does not account for the relaxation of pure hydro-static pressure. Also, the concept of individual solute pairs loses its significance in alloys with high solute concentrations. The theory assumes that the number of atom pairs remains constant.

Theory of Short-Range Order

LeClaire and Lomer have postulated a directional short-range order theory (11) to eliminate some of the drawbacks in the Zener theory. This theory applies to all compositions since it considers the two components of the alloy in a symmetrical fashion and does not

distinguish between solute and solvent atoms. A different short-range order parameter is assigned to each of the nearest-neighbor directions in the lattice when a stress is applied. The equilibrium value of short-range order in one direction relative to that in another direction changes under the application of an external stress, thus producing an anelastic relaxation.

Anisotropy of Zener Relaxation Phenomenon

In recent years, an excellent series of papers (12, 13, 14, 15) on the Zener relaxation effect has been published. One of the main objectives in this series of papers was to study the effect of anisotropy on the relaxation strength, which led to the suggestion by Seraphim and Nowick (12), that the relaxation effect involves primarily the reorientation of next-nearest neighbor atom pairs.

The anisotropy of the Zener relaxation phenomenon was determined in body-centered cubic Li-Mg and face-centered cubic Ag-Zn solid solutions by Seraphim and Nowick (14) and in face-centered cubic Al-Cu by Berry (15). The internal friction measurements were made on single crystals both in torsional and transverse vibration. Neither the pair reorientation theory of Zener nor the short-range order theory of LeClaire and Lomer can satisfactorily explain the observed results. The pair reorientation theory and the short-range order theory, involving nearest neighbors, predict a maximum relaxation strength in the <111> direction and a minimum in the <100> direction. But, the experimental results from Seraphim and Nowick's work on Ag-Zn and Li-Mg and Berry's work on Al-Cu shows that the relaxation strength is a maximum in the <100> direction, not a minimum.

The observations may be explained fairly well by assuming that atoms in the next-nearest neighbor positions make the major contribution to the relaxation process with some contribution from nearest

neighbor pairs. This is a more general type of theory of which the pair-reorientation and directional ordering theories are special cases. It predicts that the relaxation strength is a maximum in the <100> direction and a minimum in the <111> direction for both face-centered cubic and body-centered cubic lattices which is in agreement with experimental observations. The theory also explains why the anisotropy ratio is larger in the FCC alloys than in the BCC alloys. In the FCC lattice the anisotropy of the nearest neighbor contribution is in the same direction as that of the next-nearest neighbor, but is in the opposite direction for the BCC lattice. It is not clearly understood why the next-nearest neighbor atom pairs should contribute more to the relaxation effect than nearest neighbor pairs.

In view of this, it might be proposed that a more complex configuration of three or more atoms which are nearest neighbors may be the controlling mechanism in the Zener relaxation effect. However, it has been shown that the relaxation strength varies as the square of the concentration of the solute and solvent. This rules out groupings of three or more similar atoms since their frequency of occurrence depends on the third and successively higher powers of the solute or solvent concentrations. Thus, the Zener relaxation phenomenon is still thought to be controlled by an atom pair interaction.

De Jong's Modification

The pair reorientation theory of Zener was modified by De Jong (16) to explain the orientation dependence of the relaxation strength in FCC alloys. De Jong maintains that the greatest distortion around a pair of solute atoms is along the <100> direction perpendicular to the pair axis. As shown in Fig. 3a, the greatest distortion of the four common nearest neighbors (positions A, B, C, and D) around a pair of solute atoms (positions E and F) affects primarily the <100> direction

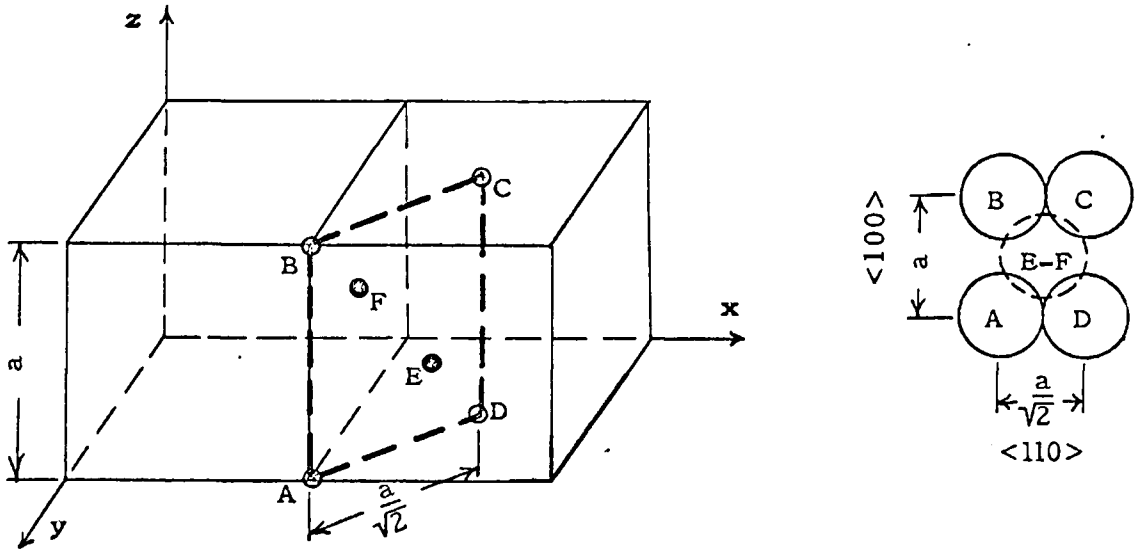

(a)

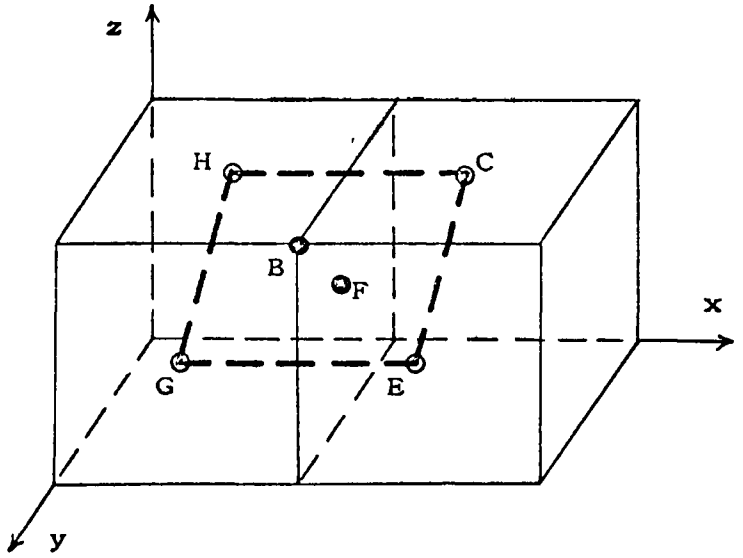

(b)

Fig. 3.--De Jong's model for stress induced ordering in FCC substitutional alloys. Fig. 3a shows a pair of solute atoms E and F with four common nearest neighbors A, B, C, and D. Greatest distortion of the lattice is in the z direction (<100> direction). Fig. 3b shows the new positions after the solute atom jumps from E to B. Greatest distortion is now in the x direction (<100> direction).

("a" dimension) rather than the <110> direction ($a/\sqrt{2}$ dimension). Thus, the greatest distortion in the lattice is in the z direction (a <100> direction) in Fig. 3a. If the solute atom in position F jumps to position B, then the four common nearest neighbors to the solute atoms are now positions C, E, G, and H as shown in Fig. 3b. The maximum strain of the lattice has rotated to the x direction (a <100> direction). No matter what the permissible orientation of a pair of solute atoms, the maximum strain of the lattice will be a <100> direction.

Thus, a tensile stress on the lattice favors the rotation of solute pairs, so that their axis is perpendicular to the <100> direction most closely aligned with the tensile stress. The three possible <100> directions for maximum strain will be equally inclined to the <111> directions. Therefore, the relaxation strength will be a maximum in the <100> direction and a minimum in the <111> direction. This agrees with the results obtained on single crystals of Ag-Zn (14) and Al-Cu (15). The distortion around second and third nearest neighbor solute pairs will contribute very little to the Zener relaxation in a particular direction.

Summary

Suggested mechanisms for the Zener relaxation involve atomic migration, a process similar to volume diffusion. Therefore, it is reasonable to expect that the activation energies for the two processes might be nearly the same. This has been substantiated in several alloy systems, but discrepancies do exist. For example, activation energies obtained from diffusion studies and internal friction experiments in the Cu-Zn system (2) have not agreed. The purpose of the present work is to compare the activation energy obtained from internal friction measurements on an alpha brass alloy with diffusion data to help clarify inconsistencies which exist in the Cu-Zn system.

EXPERIMENTAL PROCEDURE

Anelastic measurements were made on an alpha brass alloy with a composition of 13 at. % zinc - 87 at. % copper. Wire specimens of the alloy were used to make low-frequency internal friction and elastic after-effect measurements.

Specimen Preparation

Specimens used for the internal friction studies were wires 10 inches in length and 0.032 inches in diameter (17). An ingot of about 15 at. % zinc - 85 at. % copper was prepared by melting spectrographically pure metals in a high-purity graphite crucible. The graphite crucible with a screw-in cap was machined from reactor grade graphite and cleaned by boiling in aqua regia over a water bath for 3 hours (18). The crucible was leached for 6 hours in distilled water which was changed every 2 hours. It was then placed in a drying oven at 200°C for 2 hours and afterwards heated to 900°C in a vacuum for 20 minutes. High purity zinc and copper were placed in the crucible which was then sealed off under vacuum in a vycor capsule 8 inches in length and 1-1/8 inches in diameter. The capsule was heated to 1100°C for 1 hour in a closed end tube furnace to melt the alloy. The resulting ingot, which was 1/2 inch in diameter and about 5 inches in length, was swaged and drawn into 0.032 inch diameter wire by Engelhard Industries, Inc.

Specimens 10 inches in length were cut from the center of the as-drawn wire with samples taken between each specimen for chemical analyses. The composition of the samples cut from between the specimens to be used for the internal friction studies had a composition of 13 at. % zinc -87 at. % copper. The wire specimens were sealed off in evacuated vycor tubing and given recrystallization anneals for various times at temperatures ranging from 400°C to 900°C. The lowest

annealing temperature gave a very fine grain size, while the highest annealing temperature produced a grain size equal to the diameter of the wire. Certain wire specimens were then selected for internal friction measurements

Low-Frequency Internal Friction Measurements

An inverted torsion pendulum apparatus was used to make low-frequency internal friction measurements at about 1 cycle per second (1, 17). A special tube furnace with an inverted torsion pendulum was constructed as shown in Fig. 4. The furnace was built by winding a ceramic tube with two windings of nichrome wire. An evenly spaced winding was placed onto the furnace tube and coated with alundum cement. A second winding spaced closely on the ends was placed over the first winding. Each winding was controlled individually with a variac so that an even temperature gradient could be obtained over the length of the test specimen. The temperature was measured by three chromel-alumel thermocouples placed in the furnace so as to correspond with the middle and ends of a test specimen. The temperature was controlled within $\pm 2^{\circ}C$ during an internal friction measurement.

The inverted torsion pendulum consisted of two pin vises, one welded to a steel rod and held rigid at the bottom of the furnace, the other welded to a steel rod with a moment arm and mirror. The upper pin vise and torsion pendulum were counter-balanced over a pulley arrangement. The pendulum arm had movable weights to vary the moment of inertia, thus changing the frequency of vibration. The ends of the torsion bar were threaded with small nuts for fine adjustment to balance the pendulum. Two electromagnets were positioned so that when an electric current was pulsed through the electromagnets, the pendulum would be set in torsional oscillation. A narrow light-slit source was focused on the mirror of the pendulum arm and reflected to

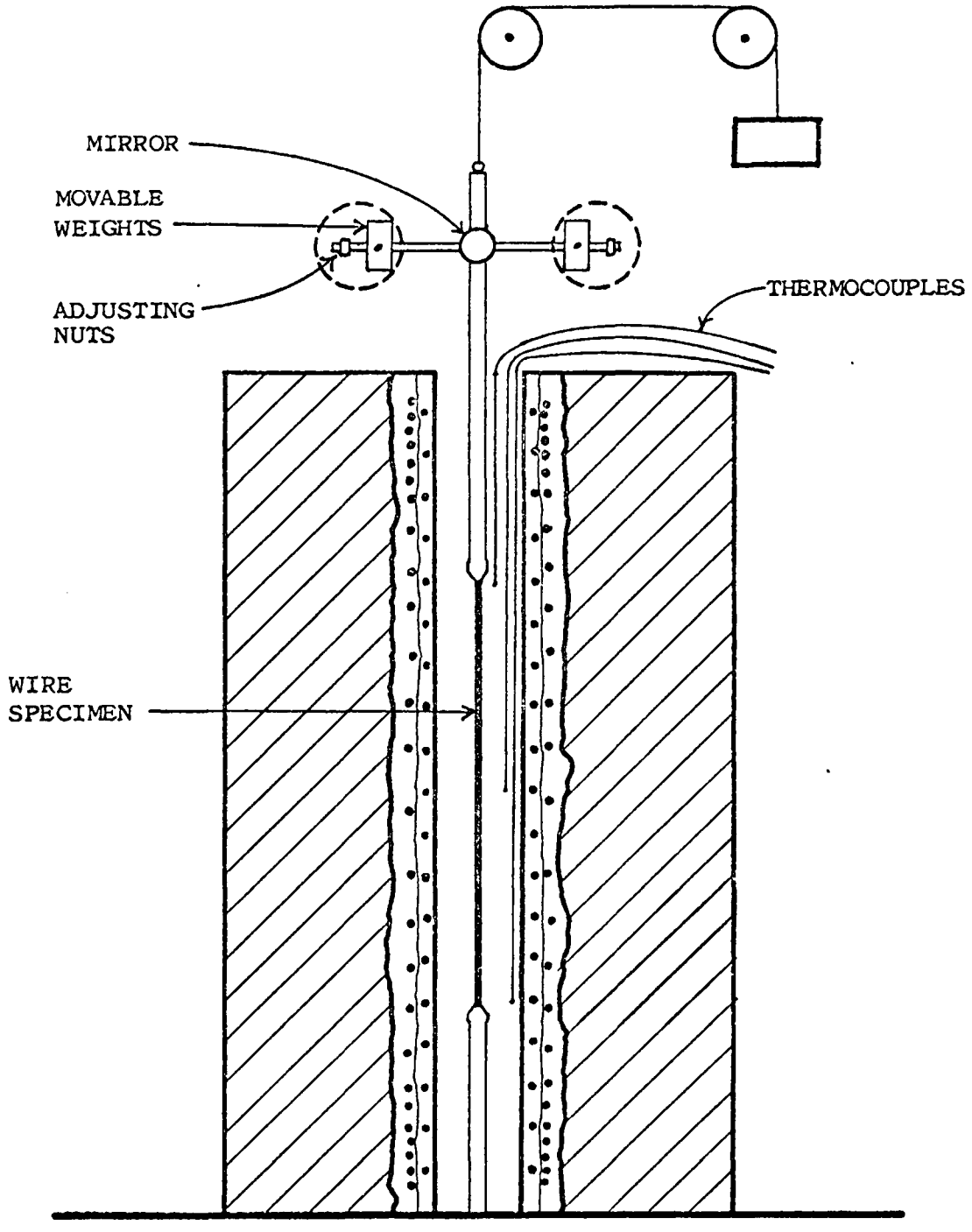

Fig. 4.--Schematic diagram of inverted torsion pendulum and furnace apparatus.

a translucent scale located 2.6 meters away from the mirror. With this arrangement, visual observations of the oscillations could be made at vibrational periods of about one cycle per second.

During internal friction measurements on a specimen, the maximum amplitude of vibration used was 8 cm, which produced a maximum shearing strain on the surface of the test wire of 5×10^{-5}. The damping was independent of the amplitude of oscillation and the time was recorded for the amplitude to decay to one-half its value. The period of vibration was determined by counting the number of oscillations for a period of time. Using Eqn.[11] the internal friction was calculated at various test temperatures to yield a plot of internal friction versus temperature.

Elastic After-Effect Measurements

The elastic after-effect was used to measure relaxation times on the order of 100 to 1000 seconds (7,19). The apparatus used for the low-frequency internal friction measurements was modified slightly to measure the elastic after-effect. The moment arm was removed from the pin vise gripping the wire specimen. The wire was twisted through an angle of about 10° and held there for a time much longer than the expected relaxation time. When the pin vise was released, the angular deflection did not return all the way to zero. There was an instantaneous recovery of the elastic strain, but the anelastic strain decayed gradually to zero with time. The strain, which is expressed by Eqn. [13], was measured as a function of time for a particular temperature. The relaxation time was determined by plotting strain versus log time and using the value of the time at the inflection point.

EXPERIMENTAL RESULTS

Relaxation times for the Zener effect in the alpha brass alloy were measured over a range of about 1 to 4 x 10^3 seconds. This spread in relaxation time corresponded to a temperature range of 225°C to 355°C. The data were fitted with the Arrhenius equation to obtain the activation energy for the stress induced ordering process.

Low Frequency

Internal friction measurements were made on a number of wire specimens which had been given recrystallization heat treatments at varying times and temperatures. The results of some preliminary internal friction measurements on two wire specimens are shown in Fig. 5. One wire was annealed at 400°C for 30 minutes in situ in the torsion pendulum furnace. The resulting internal friction curve was obtained on cooling from 400°C to room temperature. The value of the internal friction decreased rapidly with decreasing temperature. No internal friction peak was obtained. It appears that the curve was on the low temperature side of a grain boundary relaxation peak which would mask the Zener relaxation peak. Metallographic examination of this specimen showed that it was in the initial stages of recrystallization.

A second wire was annealed at 700°C for 1 hr. The internal friction curve obtained from this specimen had a peak in the neighborhood of 500°C. This peak was believed to be caused by grain boundary relaxation, since the grain size was about one half the wire's diameter. No further investigation was done on this peak. The contribution of internal friction due to the grain boundaries still seemed to be masking the Zener peak.

Other wire samples were annealed at 800°C and 900°C to obtain larger grain sizes. Wires annealed at 900°C had a grain size equal to the wire diameter and were used for internal friction measurements.

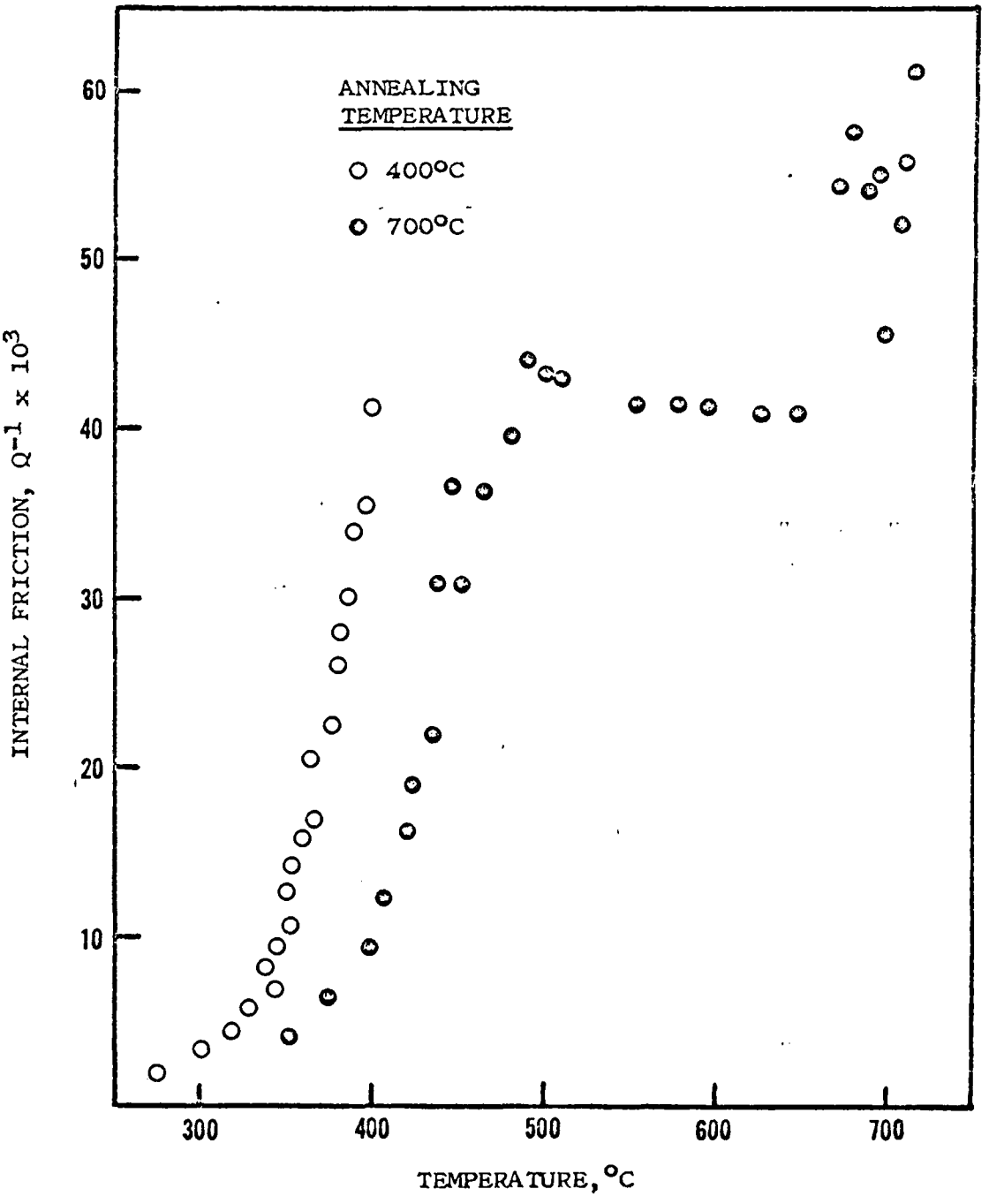

Fig. 5.--Variation of internal friction with temperature for alpha brass wires annealed at 400°C and 700°C. Frequency of vibration about 1 cycle per second.

The results of internal friction measurements for two typical wire samples annealed at 900°C for 36 hours and 87 hours are shown in Figs. 6 and 7, respectively, Both internal friction curves exhibit a Zener relaxation peak. The same curve was obtained on heating as on cooling for the internal friction measurements on all wire specimens. The internal friction curves were corrected for background damping as shown in Fig. 7 by subtracting the background damping (dotted line) from the internal friction curve.

The position of the peaks shifted to lower temperatures with a lower frequency of specimen oscillation. The maximum peak height for the wire in Fig. 6 occurred at 350°C with a frequency of 1.1 cycles per second. In Fig. 7 the peak shifted to 338°C with a frequency of 0.65 cycles per second. A total of six relaxation times was measured at a frequency of about 1 cycle per second. These results are summarized in Table 1.

Attempts were also made to determine the inflection point for the change in the elastic modulus. However, the measurements of the frequency of vibration were not accurate enough to yield a suitable plot of temperature versus the frequency squared.

Elastic After-Effect

The relaxation times for several temperatures were obtained from the elastic after-effect measurements. The relaxation time at a particular temperature was determined from the inflection point of a plot of log time versus linear strain. Typical elastic after-effect curves for two temperatures are shown in Fig. 8. The time of relaxation increased with decreasing temperature. The relaxation times for a total of seven elastic after-effect measurements are summarized in Table 2.

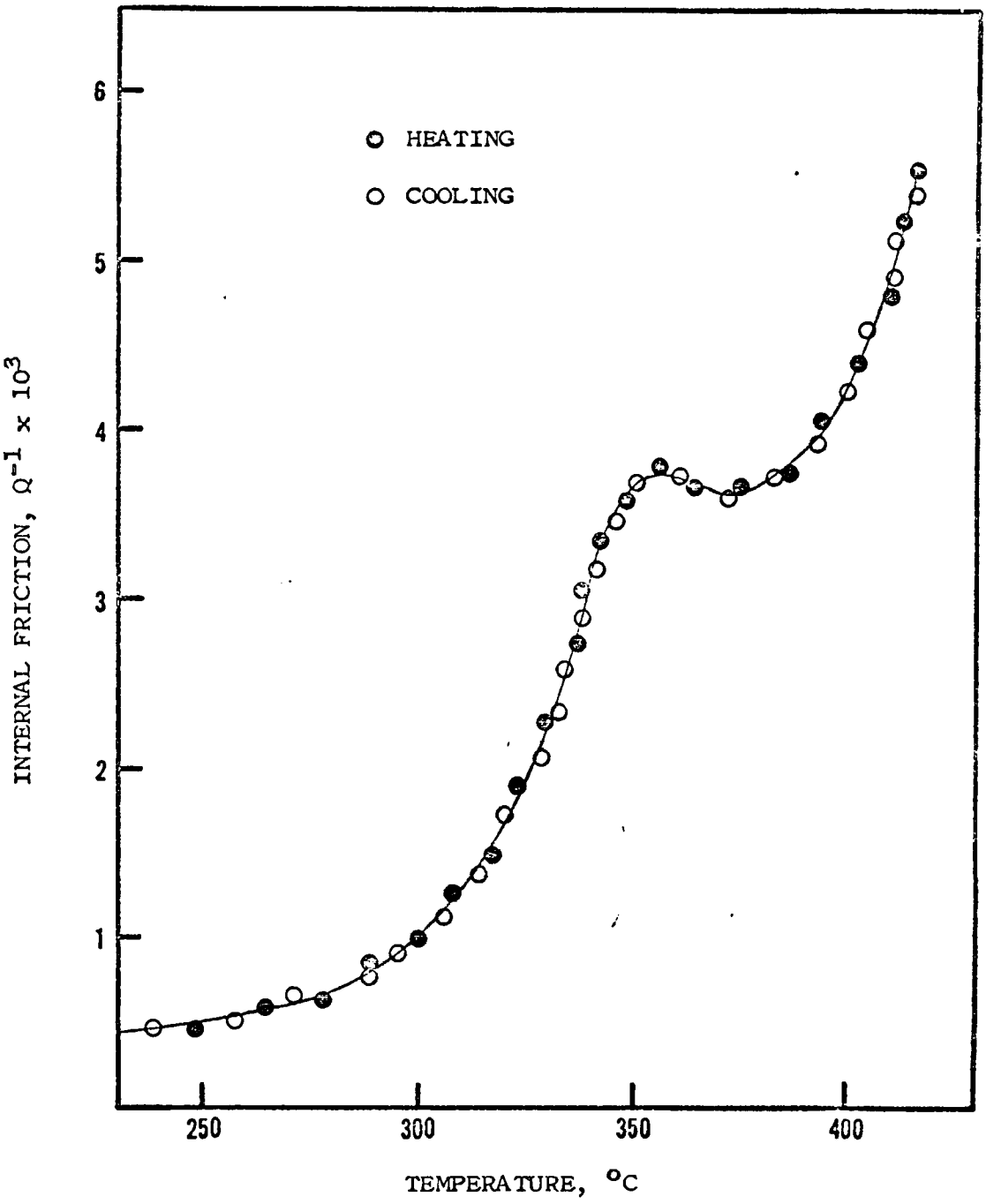

Fig. 6.--Variation of internal friction with temperature for an alpha brass wire annealed at 900°C for 36 hrs. Temperature of peak (corrected for background damping) was 350°C. Frequency of vibration at peak was 1.1 cycles per second.

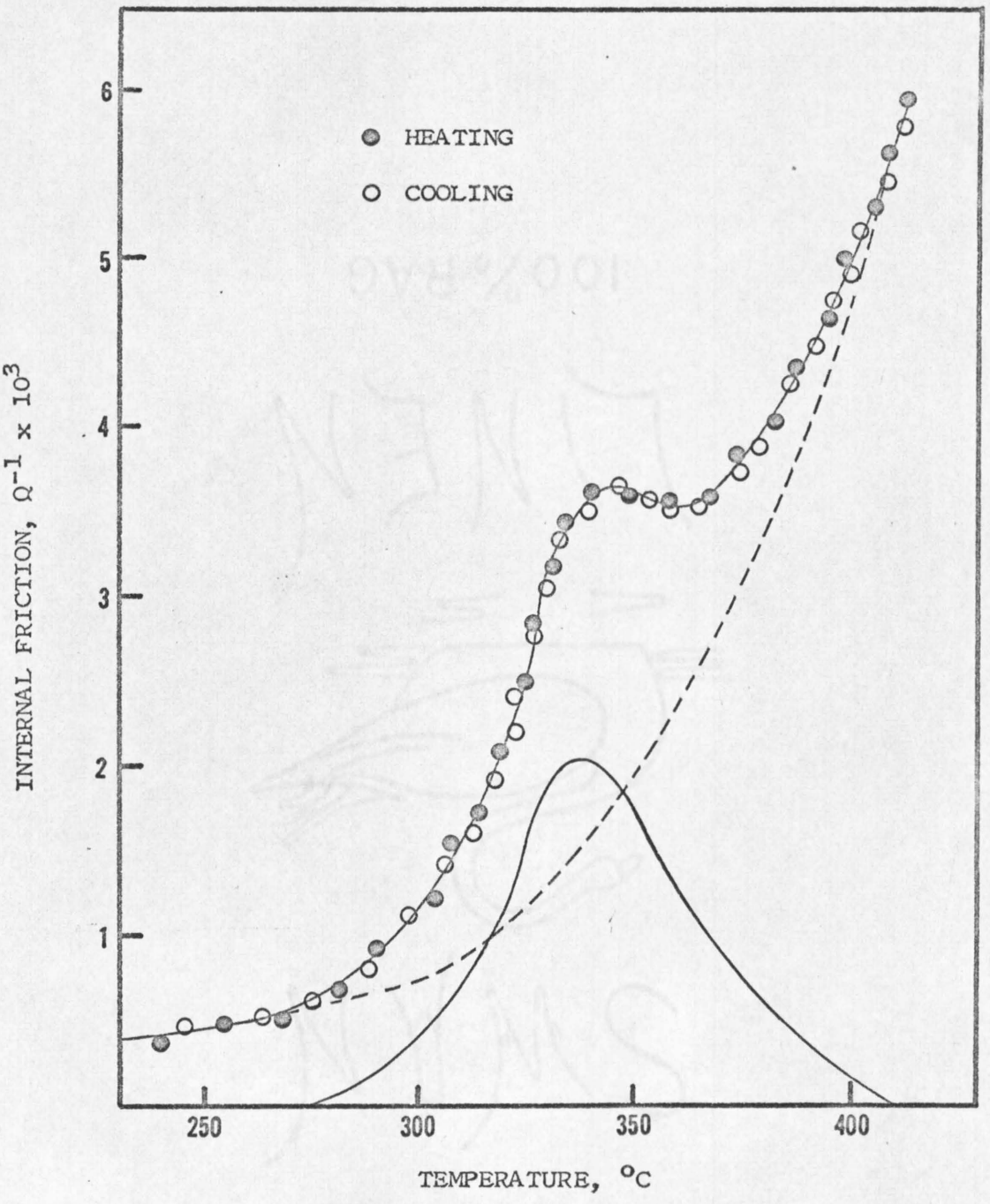

Fig. 7.--Variation of internal friction with temperature for an alpha brass wire annealed at 900°C for 87 hrs. Temperature of peak (corrected for background damping) was 338°C. Frequency of vibration at peak was 0.65 cycles per second.

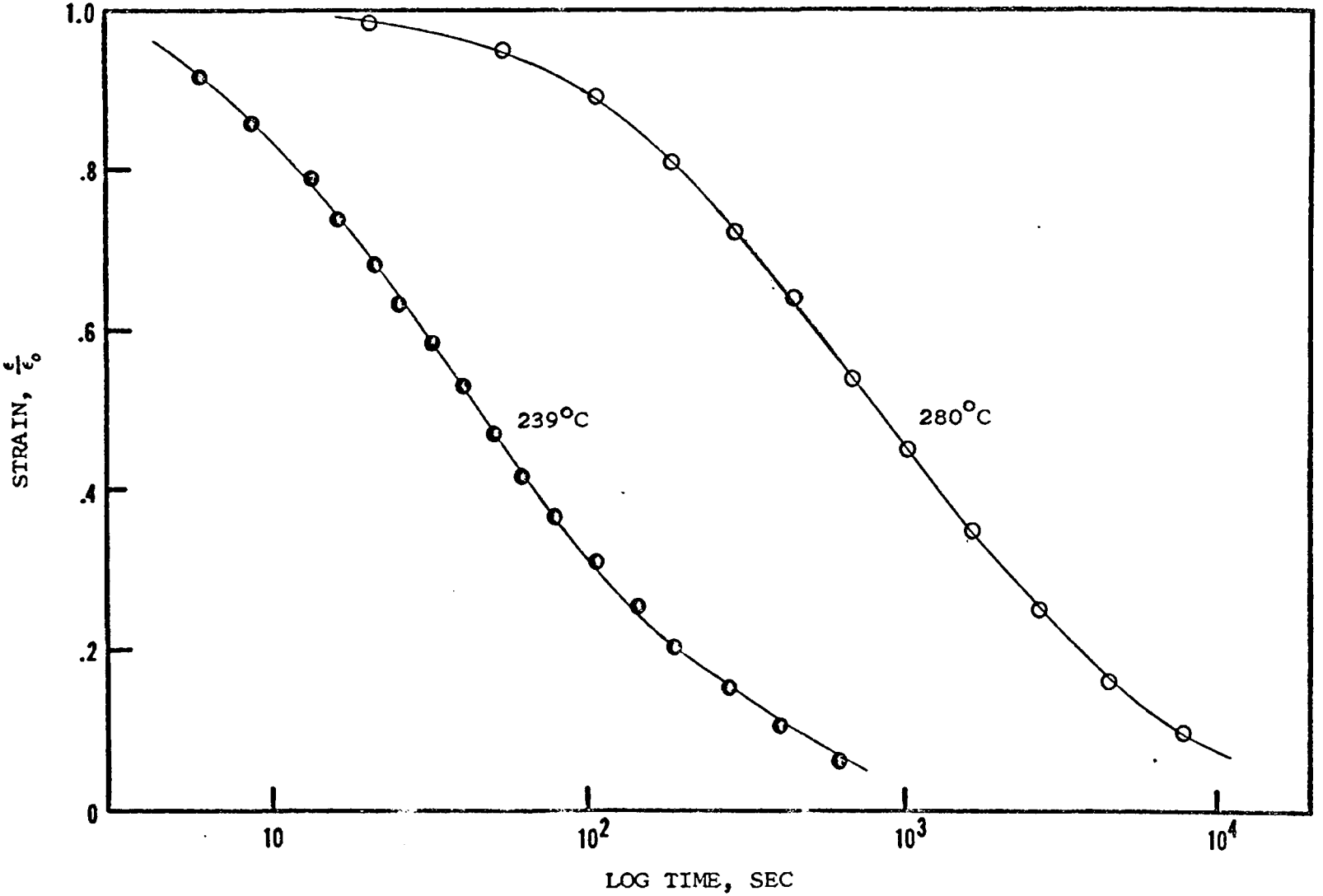

Fig. 8.--Typical elastic after-effect curves at 239°C and 280°C for the alpha brass alloy.

TABLE 1

RELAXATION TIMES FOR LOW FREQUENCY INTERNAL FRICTION MEASUREMENTS

Frequency, ω, (at peak) cycles/sec	Temperature °C	Relaxation time, τ sec
1.69	356	0.59
1.25	354	0.80
1.10	351	0.91
1.10	350	0.91
0.77	344	1.30
0.65	338	1.54

TABLE 2

RELAXATION TIMES FOR
ELASTIC AFTER-EFFECT MEASUREMENTS

Temperature °C	Relaxation time, τ sec
280	50
265	150
256	380
251	430
239	1100
232	1700
224	4700

Activation Energy

The data from the anelastic measurements were fitted with an Arrhenius equation (Eqn. [12]). The log of the relaxation time was plotted as a function of the reciprocal of absolute temperature as shown in Fig. 9. The data points were fitted with a straight line, using the least squares method.

The activation energy, obtained from the slope of the graph in Fig. 9, was 40.9 ±0.4 kcal/mole. The value of the constant τ_o, determined from the intercept, was 4.0×10^{-15} sec.

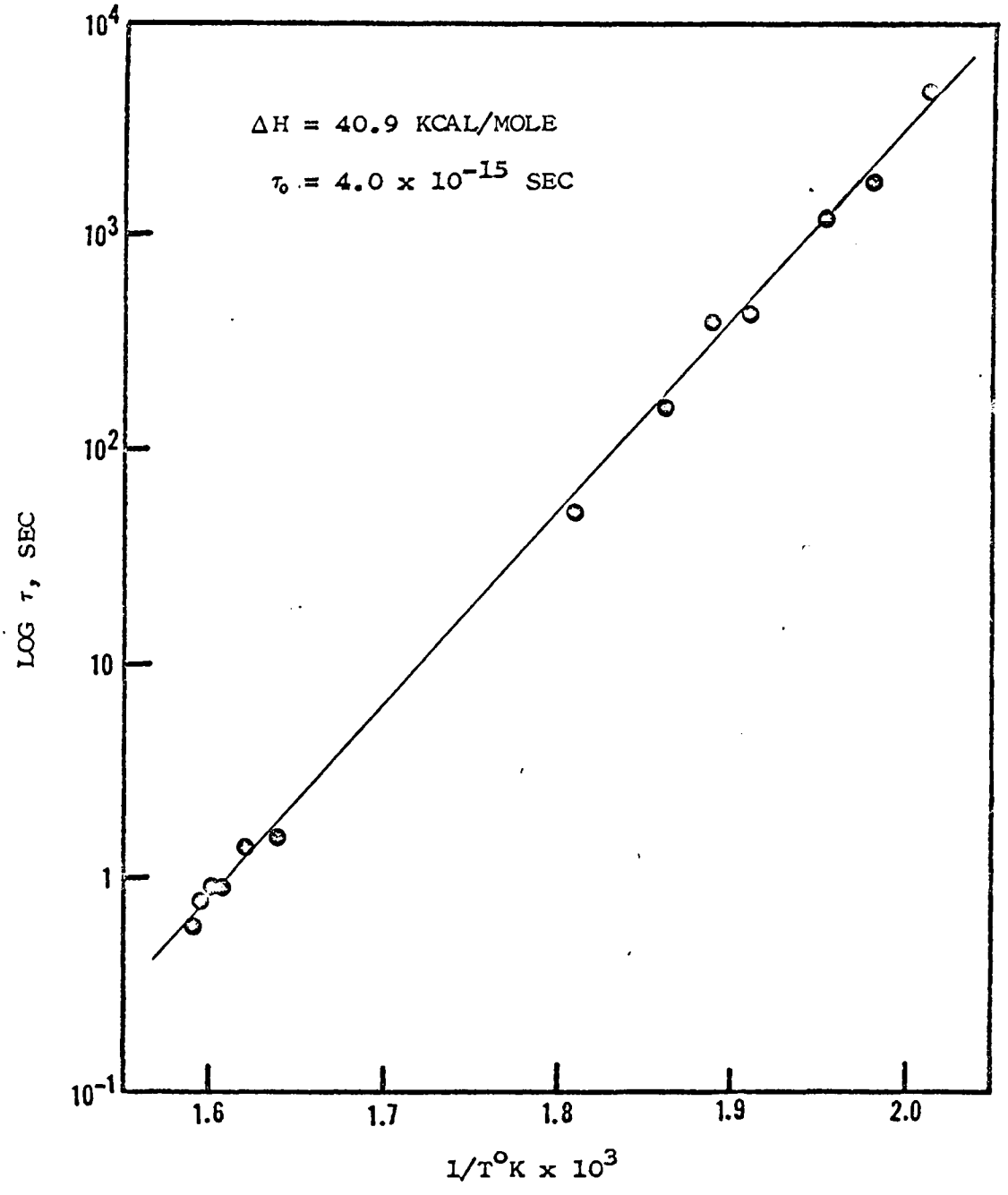

Fig. 9.--Relaxation time as a function of temperature for the anelastic measurements on the 13 at. % Zn-87 at. % Cu alloy.

DISCUSSION

It is evident from past experimental work that the mechanism giving rise to the Zener relaxation phenomenon involves some form of stress-induced ordering, although the exact model for the mechanism has not been clearly understood. The mechanism is similar to diffusion and appears to be controlled by atomic movements within the crystal lattice. The anelastic effect is only observed in alloys and its magnitude is a function of the square of the concentration and the deviation from Vegard's law. The effect is observed in well-annealed alloy single crystals and is not structure sensitive. Therefore, it is unlikely that the mechanism is related to dislocations, grain boundaries or other such defects. Based on the width of the internal friction peak, the relaxation phenomenon appears to have a single relaxation time, which implies a unique process indicating a bulk or volume property of the lattice. The heat of activation for the process, in most cases, is nearly the same as that for volume diffusion, which is to be expected if the process is controlled by atomic migration.

The purpose of the present experimental work was to compare the results obtained from anelastic measurements of the Zener relaxation with available data from diffusion experiments on alpha brass to determine if the two processes are similar. Several internal friction investigations have been made to correlate the results with diffusion data. A summary of the data from these investigations is given in Table 3.

Hino et. al, conducted a comprehensive study of tracer diffusion and anelastic measurements in 31 at. % Zn alpha brass alloys (2). The activation energy of 37.8 kcal/mole obtained for the anelastic measurements was several kcal/mole less than those observed for the tracer diffusion of either zinc or copper in the alloy. The value agreed more

closely with the activation energy for chemical diffusion of zinc in alpha brass.

Internal friction measurements were made on several alpha brass alloys by Childs and LeClaire (20). The activation energies, which are listed in Table 3, were interpolated to give an activation energy of 41.7 kcal/mole for a 13 at. % Zn-87 at. % Cu alloy. The value obtained in this study was 40.9 kcal/mole. The difference in activation energy is within experimental error for the two investigations. The results from Childs and LeClaire agreed favorably with those from Hino et al.

Other internal friction investigations have been conducted on alpha brass by Ke and Zener. Ke obtained an activation energy of 40 kcal/mole for a 29 at. % alpha brass alloy (21). This value seems to be high when compared with the results of other investigations. Zener obtained an activation energy for a 30 at. % Zn alpha brass alloy of 33.6 kcal/mole which appears to be very low compared to other results (8).

The next step was to compare the activation energies for diffusion data with the activation energy obtained in this study. There is an abundant amount of information in the literature on diffusion in the alpha brass system. The results of a few investigations are summarized in Table 4 for diffusion at 13 at. % Zn - 87 at. % Cu concentration.

Resnick and Balluffi obtained an activation energy of 40.8 kcal/mole for the interdiffusion coefficient (22). This agrees very well with the present results. None of the activation energies for diffusion obtained by other investigators (23, 24) agree with the result for this study.

An examination of diffusion information reveals that there is as much scatter in the activation energy values for diffusion at a particular composition as there is for anelastic measurements. Due to these differences in activation energies, one cannot draw any sound conclusion about whether the mechanism for the Zener relaxation process is the same as that for diffusion. However, it does appear that the activation energies determined from anelastic experiments are in the same range

TABLE 3

SUMMARY OF ACTIVATION ENERGIES FOR ANELASTIC MEASUREMENTS ON THE ALPHA BRASS SYSTEM

Reference	Composition at. % Zn	$\tau_o \times 10^{15}$ sec	ΔH kcal/mole
Hino et. al. (2)	31.7	0.86	37.8
Childs & LeClaire (20)	10.9	1.8	42.3 ± 3
	13.0		41.7*
	14.5	2.45	41.3 ± 1.5
	20.0	3.2	39.5 ± 1.0
	24.8	5.0	37.6 ± 0.6
	29.0	6.2	37.3 ± 1.0
Ke (21)	29.0		40.0 ± 2.0
Zener (8)	30.0		33.6

*Determined by interpolation

TABLE 4

SUMMARY OF ACTIVATION ENERGIES FOR DIFFUSION AT 13 at. % Zn IN THE ALPHA BRASS SYSTEM

Reference	Type of Diffusion Coefficient	ΔH kcal/mole
Resnick & Balluffi (22)	Interdiffusion ($\tilde{D}$)	40.8
Horne & Mehl (23)	Interdiffusion ($\tilde{D}$)	38.7
	Intrinsic (D_{Zn})	38.7
	Intrinsic (D_{Cu})	42.3
Da Silva & Mehl (24)	Interdiffusion ($\tilde{D}$)	42.0

as those for diffusion experiments on the alpha brass system. Therefore, it seems reasonable to use anelastic measurements to extend diffusion data to lower temperatures.

CONCLUSION

Although the present experimental work in no way clarifies the mechanism by which the Zener relaxation process takes place, the activation energy is in the same range as those obtained from diffusion studies. An activation energy of 40.9 kcal/mole was measured for the stress-induced ordering process in a 13 at. % Zn - 87at. % Cu alpha brass alloy. Therefore, based on this evidence, it appears that the stress-induced ordering process is closely related to the diffusion process. Thus, anelastic measurements can be used to extend diffusion data to lower temperatures in the alpha brass system.

RECOMMENDATIONS

Throughout the course of the experimental work there were noted a number of instances whereby the experimental procedure or technique could have been improved upon. These suggestions are given below for the benefit of future investigators conducting experimental work in this area of research.

Considerable difficulty was encountered in trying to obtain an internal friction peak for the Zener relaxation effect. Although the wire specimens were annealed at fairly high temperatures for long periods of time to give large grain size, there still appeared to be some masking of the Zener peak due to internal friction caused by grain boundaries. The grain size should be greater than the diameter of the wire so that it acts like a single crystal to minimize the internal friction contribution of grain boundaries. Larger grain size could be produced in the wire samples by using some technique such as strain annealing to promote grain growth or passing the wire sample through a Bridgman furnace to grow large grains.

Several improvements could have been made to the torsional pendulum apparatus to give better experimental results. The apparatus should be enclosed in an evacuated system to reduce background damping of the torsion pendulum; however, difficulty may be encountered in the alpha brass system due to the possible evaporation of zinc which has a high vapor pressure. Such a system could be purged with an inert atmosphere to prevent any oxidation of the sample but it was not felt that this was a problem (25). The inverted torsion pendulum worked very well, but it was very susceptible to transverse vibrations. These transverse vibrations could be reduced by constructing a special oil damping pot or by some eddy current damping technique. The placing

of the apparatus in a closed system would also have reduced vibration due to air movements. For the elastic after-effect measurements, a damping vane in an oil pot should be made to quickly dampen out rotational vibrations.

The furnace for the internal friction apparatus should be modified to permit easier and better temperature control of the wire specimen. Better temperature control could have been maintained by building a dummy specimen with pin vise holders into the furnace to be used for temperature control and measurement. Three thermocouples could be attached to the dummy sample at each end and in the center for automatic temperature control instead of variacs. A second set of three thermocouples could be attached in the same place as the three control couples so that the temperature could be read out on a potentiometer or a multipoint recorder for accurate temperature measurement.

APPENDIX A

The "standard linear solid" approximates real solids to a certain extent (3). When a constant force is suddenly applied, there is an instantaneous deformation, followed by a gradual displacement with time. Removing the force results in an instantaneous recovery in deformation, followed by a gradual recovery of the remaining deformation with time. This behavior is described by the following equation

$$a_1\sigma + a_2\frac{d\sigma}{dt} = b_1\varepsilon + b_2\frac{d\varepsilon}{dt} \qquad [A\text{-}1]$$

where σ is the stress, ε is the strain, t is the time, and a_1, a_2, b_1, and b_2 are constants. Eqn. [A-1] can be rearranged by factoring b_1 out of the right hand side and dividing through by a_1, to give

$$\sigma + \frac{a_2}{a_1}\frac{d\sigma}{dt} = \frac{b_1}{a_1}\left(\varepsilon + \frac{b_2}{b_1}\frac{d\varepsilon}{dt}\right) \qquad [A\text{-}2]$$

Three new independent constants may be defined as follows

$$\tau_\varepsilon = \frac{a_2}{a_1}, \qquad \tau_\sigma = \frac{b_2}{b_1}, \qquad M_R = \frac{b_1}{a_1}$$

where τ_ε is the relaxation of stress under constant strain, τ_σ is the relaxation of strain under constant stress, and M_R is the relaxed elastic modulus. Substituting these new constants in Eqn. [A-2] yields

$$\sigma + \tau_\varepsilon\frac{d\sigma}{dt} = M_R\left(\varepsilon + \tau_\sigma\frac{d\varepsilon}{dt}\right) \qquad [A\text{-}3]$$

which is Eqn. [2] in the text. It is of interest to examine Eqn. [A-3] under conditions of constant stress or strain.

Under a condition of constant stress as shown in Fig. 1a

$$\frac{d\sigma}{dt} = 0 \quad \text{and} \quad \sigma = \sigma_o$$

Eqn. [A-3] becomes

$$\sigma_o = M_R \left(\varepsilon + \tau_\sigma \frac{d\varepsilon}{dt}\right) \qquad [A\text{-}4]$$

Rearranging and integrating

$$M_R \tau_\sigma \frac{d\varepsilon}{dt} = \sigma_o - M_R \varepsilon \qquad [A\text{-}5]$$

$$M_R \int \frac{d\varepsilon}{\sigma_o - M_R \varepsilon} = \frac{1}{\tau_\sigma} \int dt \qquad [A\text{-}6]$$

gives

$$-\ell n(\sigma_o - M_R \varepsilon) = \frac{t}{\tau_\sigma} + C_1 \qquad [A\text{-}7]$$

where C_1 is a constant of integration. Taking the antilogarithm gives

$$\sigma_o - M_R \varepsilon = C_2 e^{-t/\tau_\sigma} \qquad [A\text{-}8]$$

where C_2 is a constant. At time, $t = 0$, the initial value of strain is $\varepsilon = \varepsilon_o$. Thus, $C_2 = \sigma_o - M_R \varepsilon_o$ which is substituted in Eqn. [A-8] gives

$$\sigma_o - M_R \varepsilon = (\sigma_o - M_R \varepsilon_o) e^{-t/\tau_\sigma} \qquad [A\text{-}9]$$

Solving for ε yields

$$\varepsilon = \frac{\sigma_o}{M_R} + \left(\varepsilon_o - \frac{\sigma_o}{M_R}\right) e^{-t/\tau_\sigma} \qquad [A\text{-}10]$$

which gives the strain as a function of time under a constant stress. Eqn. [A-10] corresponds to Eqn. [3] in the text. At infinite time $\varepsilon_\infty = \sigma_o / M_R$.

If the strain is constant as shown in Fig 1b, then

$$\frac{d\varepsilon}{dt} = 0 \quad \text{and} \quad \varepsilon = \varepsilon_o$$

Eqn. [A-3] becomes

$$\sigma + \tau_\varepsilon \frac{d\sigma}{dt} = M_R \varepsilon_o \qquad [A\text{-}11]$$

Rearranging and integrating

$$d\sigma = (M_R\varepsilon_o - \sigma)\frac{dt}{\tau_\varepsilon} \qquad [A\text{-}12]$$

$$\int\frac{d\sigma}{M_R\varepsilon_o - \sigma} = \frac{1}{\tau_\varepsilon}\int dt \qquad [A\text{-}13]$$

gives

$$-\ell n\,(M_R\varepsilon_o - \sigma) = \frac{t}{\tau_\varepsilon} + C_3 \qquad [A\text{-}14]$$

where C_3 is a constant of integration. Taking the antilogarithm gives

$$M_R\varepsilon_o - \sigma = C_4 e^{-t/\tau_\varepsilon} \qquad [A\text{-}15]$$

where C_4 is a constant. At time, $t = 0$, the initial value of stress is $\sigma = \sigma_o$. Thus

$$C_4 = M_R\varepsilon_o - \sigma_o$$

Substituting for C_4 in Eqn. [A-15] gives

$$M_R\varepsilon_o - \sigma = (M_R\varepsilon_o - \sigma_o)\, e^{-t/\tau_\varepsilon} \qquad [A\text{-}16]$$

Solving for σ yields

$$\sigma = M_R\varepsilon_o + (\sigma_o - M_R\varepsilon_o)\, e^{-t/\tau_\varepsilon} \qquad [A\text{-}17]$$

which gives the stress as a function of time under constant strain. Eqn. [A-17] corresponds to Eqn. [4] of the text. At infinite time, $\sigma_\infty = M_R\varepsilon_o$.

APPENDIX B

In anelastic experiments when materials are investigated under periodic loads, the strain lags behind stress (3). Under these conditions the following solutions

$$\sigma = \sigma_o e^{i\omega t} \text{ and } \varepsilon = \varepsilon_o e^{i\omega t}$$

where i is imaginary, t is the time, and ω is the angular frequency of oscillation, are substituted in Eqn. [2] of the text to give

$$(1 + i\omega\tau_\varepsilon)\sigma_o = M_R(1 + i\omega\tau_\sigma)\varepsilon_o \qquad [B-1]$$

The stress and strain are correlated by a complex modulus, M_ζ, giving

$$\sigma_o = M_\zeta \varepsilon_o \qquad [B-2]$$

where

$$M_\zeta = \left(\frac{1 + i\omega\tau_\sigma}{1 + i\omega\tau_\varepsilon}\right) M_R \qquad [B-3]$$

The tangent of the phase angle by which strain lags behind stress is a measure of the internal friction. The tangent of the phase angle is found by taking the ratio of the imaginary part to the real part of the complex modulus. The right hand side of Eqn. [B-3] is changed as follows

$$M_\zeta = \left(\frac{1 + i\omega\tau_\sigma}{1 + i\omega\tau_\varepsilon}\right)\left(\frac{1 - i\omega\tau_\varepsilon}{1 - i\omega\tau_\varepsilon}\right) M_R \qquad [B-4]$$

Multiplying out gives

$$M_\zeta = \left(\frac{1 + i\omega\tau_\sigma - i\omega\tau_\varepsilon + \omega^2\tau_\sigma\tau_\varepsilon}{1 + \omega^2\tau_\varepsilon^2}\right) M_R \qquad [B-5]$$

Separating into imaginary and real parts yields

$$M_\zeta = \left[\frac{1 + \omega^2\tau_\sigma\tau_\varepsilon}{1 + \omega^2\tau_\varepsilon^2}\right] M_R + \left[\frac{i\omega(\tau_\sigma - \tau_\varepsilon)}{1 + \omega^2\tau_\varepsilon^2}\right] M_R \qquad [B-6]$$

Taking the ratio of the imaginary part (second term) to real part (first term) gives the tangent of the phase angle

$$\tan \delta = \frac{\omega(\tau_\sigma - \tau_\varepsilon)}{1 + \omega^2 \tau_\sigma \tau_\varepsilon} \qquad [B-7]$$

Eqn. [B-7] can be simplified by using the geometric mean for the two relaxation times

$$\tau = \sqrt{\tau_\sigma \tau_\varepsilon} \qquad [B-8]$$

Substituting Eqn. [B-8] in Eqn. [B-7] and multiplying top and bottom of Eqn. [B-7] by τ yields

$$\therefore \tan \delta = \left[\frac{\tau_\sigma - \tau_\varepsilon}{\tau}\right]\left[\frac{\omega\tau}{1 + (\omega\tau)^2}\right] \qquad [B-9]$$

Substituting for τ in first term of Eqn. [B-9] gives

$$\tan \delta = \left[\frac{\tau_\sigma - \tau_\varepsilon}{\sqrt{\tau_\sigma \tau_\varepsilon}}\right]\left[\frac{\omega\tau}{1 + (\omega\tau)^2}\right] \qquad [B-10]$$

$$\tan \delta = \left[\sqrt{\frac{\tau_\sigma}{\tau_\varepsilon}} - \sqrt{\frac{\tau_\varepsilon}{\tau_\sigma}}\right]\left[\frac{\omega\tau}{1 + (\omega\tau)^2}\right] \qquad [B-11]$$

Recalling Eqn. [7], $M_u/M_R = \tau_\sigma/\tau_\varepsilon$, from the text and substituting in Eqn. [B-11] gives

$$\tan \delta = \left[\sqrt{\frac{M_u}{M_R}} - \sqrt{\frac{M_R}{M_u}}\right]\left[\frac{\omega\tau}{1 + (\omega\tau)^2}\right] \qquad [B-12]$$

Combining the first term gives

$$\tan \delta = \left[\frac{M_u - M_R}{M_R M_u}\right]\left[\frac{\omega\tau}{1 + (\omega\tau)^2}\right] \qquad [B-13]$$

Defining

$$\Delta E = \frac{M_u - M_R}{\sqrt{M_R M_u}} \qquad [B-14]$$

which is called the relaxation strength gives

$$\tan \delta = \Delta E \frac{\omega\tau}{1 + (\omega\tau)^2} \qquad [B\text{-}15]$$

Which is Eqn. [7] in the text.

APPENDIX C

In an experimental method where an oscillating system is allowed to decay freely, the internal friction may be expressed by the logarithmic decrement (3) as

$$\tan \delta = \frac{\text{logarithmic decrement}}{\pi} \qquad [C-1]$$

The logarithmic decrement is defined as the natural logarithm of the ratio of successive amplitudes of oscillation. Therefore, Eqn. [C-1] becomes

$$\tan \delta = \frac{\ell n \frac{A_o}{A_1}}{\pi} \qquad [C-2]$$

where A_o is the amplitude of any oscillation and A_1 is the amplitude of the next successive oscillation. For each succeeding amplitude of oscillation, the logarithmic decrement is

$$\text{log. dec.} = \ell n \frac{A_o}{A_1} = \ell n \frac{A_1}{A_2} = \ldots = \ell n \frac{A_{m-1}}{A_m} \qquad [C-3]$$

where A_o, A_1, A_2, ... A_m are amplitudes of successive oscillations.

The slope of the decaying amplitude is linear when the ℓn of the amplitude is plotted versus the number of cycles. Thus, for any number, m, of cycles, the slope is

$$\text{Slope} = \frac{\ell n A_o - \ell n A_m}{t\omega} \qquad [C-4]$$

where the number of cycles is equal to the time, t, multiplied by the frequency, ω. The amplitude of the A_m cycle of oscillation is equal to some fractional value of the initial amplitude A_o. For convenience let

$$A_m = \frac{1}{N} A_o \qquad [C-5]$$

Therefore, the slope after m cycles is A_o

$$\text{Slope} = \frac{\ell n\, A - \ell n \frac{o}{N}}{t\omega} \qquad [C-6]$$

or

$$\text{Slope} = \frac{\ell n\, N}{t\omega} \qquad [C-7]$$

For one cycle, m = 1, and the slope would be

$$\text{Slope} = \frac{\ell n\, A_o - \ell n\, A_1}{1} \qquad [C-8]$$

or

$$\text{Slope} = \ell n \frac{A_o}{A_1} \qquad [C-9]$$

Thus, equating Eqns. [C-7] and [C-9] gives

$$\ell n \frac{A_o}{A_1} = \frac{\ell n\, N}{t\omega} \qquad [C-10]$$

Substituting in Eqn. [C-2] yields

$$\tan \delta = \frac{\ell n\, N}{\pi \omega t} \qquad [C-11]$$

which is Eqn. [12] in the text.

REFERENCES

(1) Wert, C.A. Modern Research Techniques in Physical Metallurgy. Cleveland: American Society for Metals, 1953, pp. 225-250.

(2) Hino, J., Tomizuka, C., and Wert, C. Acta Metallurgica, Vol. 5 (1957) p. 41.

(3) Zener, C. Elasticity and Anelasticity of Metals. Illinois: The University of Chicago, 1948.

(4) Van Bueren, H.G. Imperfections in Crystals. Amsterdam: North-Holland Publishing Company, (1961), pp. 348-403.

(5) Entwistle, K.M. Metallurgical Reviews, Vol. 7 (1962) p. 175.

(6) Nowick, A.S. Progress in Metal Physics, Vol. 4 (1961) p. 1

(7) Nowick, A.S. Physical Review, Vol. 88 (1952) p. 925.

(8) Zener, C. Transactions AIME, Vol. 152 (1943) p. 122.

(9) Zener, C. Physical Review, Vol. 71 (1947) p. 34.

(10) LeClaire, A.D. Philosophical Magazine, Vol. 42 (1951), p. 673.

(11) LeClaire, A.D. and Lomer, W.M. Acta Metallurgica, Vol. 2, (1954) p. 731.

(12) Nowick, A.S. and Seraphim, D.P. Acta Metallurgica, Vol. 9 (1961) p. 40.

(13) Li, C.Y. and Nowick, A.S. Acta Metallurgica, Vol. 9 (1961), p. 49.

(14) Seraphim, D.P. and Nowick, A.S. Acta Metallurgica, Vol. 9, (1961) p. 85.

(15) Berry, B.S. Acta Metallurgica, Vol. 9 (1961), p. 98.

(16) De Jong, M. Acta Metallurgica, Vol. 10 (1962) p. 334.

(17) Ke, T.S. Physical Review, Vol. 71 (1947) p. 533.

(18) Slifkin, L., Lazarus, D., and Tomizuka, C. Journal of Applied Physics, Vol. 23 (1952) p. 1032.

(19) Wert, C.A. Physical Review, Vol. 79 (1950) p. 601.

(20) Childs, B.G. and LeClaire, A.D. Acta Metallurgica, Vol. 2 (1954) p. 718.

(21) Ke, T.S. Journal of Applied Physics, Vol. 19 (1948) p. 285.

(22) Resnick, R. and Balluffi, R.W. Transactions AIME, Vol. 203 (1955) p. 1004.

(23) Horne, G.T. and Mehl, R.F. Transactions AIME, Vol. 203 (1955) p. 88.

(24) Da Silva, L.C. and Mehl, R.F. Transactions AIME, Vol. 191 (1951) p. 155.

(25) Rotherham, L. and Pearson, S. Transactions AIME, Vol. 206 (1956) p. 881.